Journal of Hazardous Materials 209–210 (2012) 204–217

Contents lists available at SciVerse ScienceDirect

Journal of Hazardous Materials

journal homepage: www.elsevier.com/locate/jhazmat

Feasibility of flare gas reformation to practical energy in Farashband gas refinery: No gas flaring

Mohammad Reaza Rahimpour[a,b,*], Seyyed Mohammad Jokar[a]

[a] Department of Chemical Engineering, School of Chemical and Petroleum Engineering, Shiraz University, Shiraz 71345, Iran
[b] Gas Center of Excellence, Shiraz University, Shiraz 71345, Iran

ARTICLE INFO

Article history:
Received 13 July 2011
Received in revised form
24 December 2011
Accepted 4 January 2012
Available online 11 January 2012

Keywords:
Flare gas recovery
Economic evaluation
GTL technology
Electricity generation
Gas compression

ABSTRACT

A suggested method for controlling the level of hazardous materials in the atmosphere is prevention of combustion in flare. In this work, three methods are proposed to recover flare gas instead of conventional gas-burning in flare at the Farashband gas refinery. These methods aim to minimize environmental and economical disadvantages of burning flare gas. The proposed methods are: (1) gas to liquid (GTL) production, (2) electricity generation with a gas turbine and, (3) compression and injection into the refinery pipelines. To find the most suitable method, the refinery units that send gas to the flare as well as the required equipment for the three aforementioned methods are simulated. These simulations determine the amount of flare gas, the number of GTL barrels, the power generated by the gas turbine and the required compression horsepower. The results of simulation show that 563 barrels/day of valuable GTL products is produced by the first method. The second method provides 25 MW electricity and the third method provides a compressed natural gas with 129 bar pressure for injection to the refinery pipelines. In addition, the economics of flare gas recovery methods are studied and compared. The results show that for the 4.176 MMSCFD of gas flared from the Farashband gas refinery, the electricity production gives the highest rate of return (ROR), the lowest payback period, the highest annual profit and mild capital investment. Therefore, the electricity production is the superior method economically.

© 2012 Elsevier B.V. All rights reserved.

1. Introduction

1.1. Gas flaring

It is commonly accepted that with increasing the standard of living and the global population growth, the greenhouse gas emissions will undoubtedly increase during the next years [1]. To fulfill the ever-increasing global demand for oil and gas, enormous quantities of co-produced gas are flared as a waste by-product and large supplies of gas have emerged. Although this process ensures the safety of the rig by reducing the pressures in the system that is resulted from gas liberation, it is very harmful for the environment. It has been the source of much controversial debate as not only wasting a considerable amount of valuable energy but also contributing to severe environmental problems in the petroleum and related industries [2]. According to the World Bank [3], the annual volume of natural gas flared or vented in the world for the year 2003 amounted to more than 100 billion cubic meters which represents the annual gas consumption of France and Germany combined. This amount of gas flaring level has remained constant over the past 20 years. Flaring in Africa alone accounts for almost 35% of global flaring [4]. In Algeria alone flaring amounts to 5 Gm^3 [5]. With increasing awareness of the environmental impact and the ratification of the Kyoto protocol by most of the member countries, it is expected that gas flaring will not be allowed in the near future. This will require significant changes in the current practices of oil and gas production and processing [6]. The implementation of a no-flare design will have a great impact in reducing the emissions from production. There are a few works which are done on flare gas recovery. Ghazi and co-workers investigated the recovery of flare gas through crude oil stabilization by a multi-staged separation with intermediate feeds [7]. Xu et al. investigated a general methodology on flare minimization for chemical plant start-up operations via plantwide dynamic simulation [8]. Oguejiofor discussed some aspects of using GTL technology for reducing flare gas in Nigeria [9]. Zadakbar presented the results of two case studies of reducing, recovering and reusing flare gases from the Tabriz Petroleum Refinery and Shahid Hashemi-Nejad (Khangiran) Natural Gas Refinery, both in Iran [10]. Flaring produces a great number of harmful by-products such as dangerous particles, oxides of nitrogen (NO_x), sulfur oxides (SO_x),

* Corresponding author. Tel.: +98 711 2303071; fax: +98 711 6287294.
E-mail address: rahimpor@shirazu.ac.ir (M.R. Rahimpour).

0304-3894/$ – see front matter © 2012 Elsevier B.V. All rights reserved.
doi:10.1016/j.jhazmat.2012.01.017

and volatile organic compounds (VOC). CO_2 which produces the green-house effect is also produced by the combustion of gas in flare.

1.2. Environmental effects of SO_x, NO_x and VOC

Pollutants discharged from flares also, include sulfur oxides (SO_x), nitrogen oxides (NO_x) and VOC. The impacts of flare emissions therefore include the health impacts associated with exposure to these pollutants, and the ozone forming potential (and hence indirect health impacts) associated with hydrocarbon and NO_x emissions, and the greenhouse gas effects of methane and CO_2 emissions [11]. A US study (for the period of January 2001 to August 2002) of emissions from a number of oil refinery flare systems in the Bay Area Management District (California) concluded that, on an annual average basis, flare emissions were approximately 8 tons/day of total organic compounds (5 tons/day of non-methane organic compounds) and approximately 20 tons/day of SO_x (mainly sulfur dioxide). The daily emissions ranged from 2.5 to 55 tons/day of total organic compounds, and from 6 to 55 tons/day SO_x [12]. Flare emissions may therefore be a significant percentage of overall VOC and sulfur dioxide (SO_2) emissions. A smoking flare may be a significant contributor to overall particulate emissions [13,14].

Gaseous pollutants like sulfur dioxide that are once emitted into the atmosphere have no boundaries and become uncontrollable and cause acid deposition. Several toxicological/epidemiological investigations during the last few decades have shown that the effect of this gas is severe. Sulfuric and nitric oxides are the major causes of acid rain and fog which harm the natural environment and human life [15]. Also Ozone has been revealed to cause damage. Ozone is produced by the photochemical reaction of VOC and NO_x as the main components of the oxidant. The oxidant accelerates the oxidation of SO_2 and NO_x into toxic sulfuric and nitric acids, respectively. The removal of VOC and NO is very important to reduce the concentration of Ozone [16].

1.3. Environmental effects of CO_2

Flaring produces a great amount of carbon dioxide. Carbon dioxide emissions from flaring have high global warming potential and contribute to climate change. The mounting environmental pressure on the oil and gas production areas to cut CO_2 emissions is directly affecting the practice of flaring [17]. Carbon dioxide is a greenhouse gas and contributes to global warming. About 75% of the anthropogenic emissions of carbon dioxide come from the combustion of fossil fuels [18]. Thus, a reduction in emissions of greenhouse gases is a crucial issue. One way to reduce CO_2 emissions that is receiving increasing interest is carbon capture and storage. This involves capturing of CO_2 at emission sources and storing it where it is prevented from reaching the atmosphere [19]. The chemical reduction of carbon dioxide is regarded as the most effective method to reduce carbon dioxide concentration in the atmosphere [20]. Various investigations were performed to reduce carbon dioxide emissions to the atmosphere. Catalytic hydrogenation of CO_2 is one of the chemical reduction methods that can produce low grade hydrocarbons. Specifically, methanol is considered to be the most valuable product because of its use as feed stock to produce other valuable products [21]. Rahimpour investigated the conversion of CO_2 into methanol by catalytic hydrogenation as one of the most promising processes for stabilizing the atmospheric CO_2 level [22]. Elkamel and co-workers. investigated a hybrid neural network model for the simulation of a differential catalytic hydrogenation reactor of carbon dioxide to methanol [23]. Rahimpour and Mottaghi investigated simultaneous removal of urea, ammonia, and carbon dioxide from industrial wastewater via modeling and simulation of a hydrolyzer-separator loop [24]. Rahimpour and Kashkooli developed a comprehensive model for the absorption of carbon dioxide into promoted hot potassium carbonate solution [25].

The low quality gas that is flared releases many impurities and toxic particles into the atmosphere during the flaring process. Acidic rain, caused by sulfur oxides in the atmosphere, is one of the main environmental hazards which results from this process [6]. According to research performed by the World Bank's Global Gas Flaring Reduction Partnership (GGFR), the equivalent of almost one third of Europe's natural gas consumption is burned in flares each year which contributes to about 400 million tons of carbon dioxide emission to the atmosphere (roughly 1.5% of the global CO_2 emissions) [26]. The implementation of a no-flare design will have a great impact in reducing the emissions from production. Environmental and economical considerations have increased the use of flare gas recovery systems. Flare gas recovery reduces noise and thermal radiation, operating and maintenance costs, air pollution, gas emission, fuel gas and steam consumption. Rahimpour and Asgari investigated hydrogen production in a hydrogen perm-selective membrane reactor from purge gases of an ammonia plant [27].

1.4. GTL technology

The application of some new environmentally friendly technologies such as gas-to-liquid (GTL) technology is a good alternative for reducing gas flaring. Recently, the high oil price has created considerable interest in the development of GTL technology for the manufacture of transportation fuels. The GTL process can be a good candidate for alleviating the current oil crisis, in which synthetic liquid fuels (e.g., gasoline, diesel, and wax) are produced from stranded natural gas. This means that "stranded natural gas" in remote areas can be converted to shippable liquid fuels through the GTL process [28]. Among the various alternatives for combustion of flare gas, there has recently been an increased interest in the development of GTL technology. Such technologies play an important role in bringing gas to markets as both fuel and/or petrochemicals [29]. The GTL products have important environmental advantages compared to traditional products, giving GTL a significant edge as governments pass new and more stringent environmental legislation. In addition, refineries are faced with the challenge that crude oil is generally getting heavier, making it harder and more expensive to meet the new stringent standards. It is highly unlikely that these improvements in fuel quality can be achieved without using a technique such as blending zero sulfur GTL diesels into the current crude based product mixture. Another environmental issue is the regulatory pressure to reduce the volume of flare gas, which has serious environmental consequences. The main issue in Nigeria is to gather gas from more than 1000 wells by building gas collection facilities at the oilfields and constructing an extensive pipeline network to carry gas to an industrial facility where it turns into liquid for transportation [2]. In the GTL process, Fischer–Tropsch synthesis (FTS) is the key technology for converting synthesis gas (mixture of CO and H_2) to ultra-clean transportation fuels. The new GTL process based on a single stage fixed-bed FTS was developed in Iran in the Research Institute of Petroleum Industry (RIPI) to produce high octane and low sulfur gasoline. In this process, the modified bi-functional Fe-HZSM5 catalyst was used [30]. Marvast et al. considered a water cooled fixed-bed reactor with a length of 12 m [31]. Rahimpour and Elekaei presented a fluidized-bed hydrogen perm-selective membrane reactor for FTS where hydrogen was withdrawn from the fresh feed synthesis gas and was injected to the end segment of reactor [32]. Rahimpour and Elekaei compared the performance of fluidized-bed membrane dual-type reactor (FMDR) with conventional reactor for FTS. Results showed an enhancement in the gasoline yield along FMDR [33]. Moreover, several

investigations were performed to apply membranes in dual-type GTL reactors by Rahimpour et al. [34–38].

1.5. Electricity generation from purge gases via gas turbines

Flare gas conversion into electricity is another way for reducing flare gas. Power is a basic part of nature and it is one of the most widely used forms of energy. Although natural gas has become a key primary source of energy for electricity generation, higher fuel costs of natural gas quickly outweigh the advantages in most applications [39,40]. So flare gas from refinery could be a good candidate as a primary source. When an expansion turbine driving a generator is used, the energy in the gas can be used to generate electricity [41]. A turbine converts the kinetic energy of a moving fluid (liquid or gas) to mechanical energy. Gas turbines can be burned to produce hot combustion gases that pass directly through a turbine, spinning the blades of the turbine to generate power. There are many books on gas turbine theory, performance and gas turbine cycles notably by Walsh and Fletcher [42], Horlock [43,44], Hodge [45], Cohen et al. [46] and Kerrebrock [47]. The electric power industry evolved from a highly regulated, monopolistic industry with traditionally structured electric utilities to a less regulated, competitive industry [48]. The government opened up competition in the generation market with the creation of qualifying facilities and they removed some constraints on ownership of electric generation facilities and encouraged increased competition in the wholesale electric power business.

1.6. Compression method

Compression and transmission of gas to practical point of view is another alternative to reduce and reuse flare gas. Initially natural gas was used only in the areas in which it was produced, with excess production being vented to the air or flared. But the large demands for natural gas has developed fairly recently. The increased demand has also greatly increased the price obtained for the gas [49]. This made refineries to use flare gas recovery systems for lowering emissions by recovering flare gases before they are combusted by the flare. A flare gas recovery system compresses the flare gas for reuse in the refinery gas system [50]. A compressor is used to increase the pressure of a compressible fluid. The inlet pressure can be any value from a deep vacuum to a high positive pressure. The discharge pressure can range from sub atmospheric to high value in the tens of thousands of pounds per square inch. Compressors have numerous forms, their exact configurations being based on the application [51].

Piston compressors operate based on the displacement principle. Piston compressors are available both with one and several cylinders and also one and multiple-stage versions. Multi-cylinder compressors are used for higher outputs while multistage compressors are used for higher pressures. The gas compressed in the cylinder in the first stage (low pressure stage) is cooled in the intermediate cooler and then compressed to the final pressure in the second stage (high pressure cylinder). In single action compressors, one compression action with one rotation of the crankshaft take place while in double action compressors there are two compression actions with one rotation of the crankshaft [51].

1.7. Objective

Farashband gas refinery is one of the old and important refineries in southern part of Iran. It has been planted to dehydrate the produced gas and stabilize the accompanied condensate from Aghar and Dalan gas reservoirs. Every day about 1400 million standard cubic feet (MMscf) of gas is fed to this plant. The gas field of Aghar contains sour gas and the gas field of Dalan contains sweet gas. In summer, all of the gases from Farashband refinery are injected to the oil wells for recovery enhancement and in winter, the gas from Dalan (sweet gas) is used for general consumption and the gas from Aghar (sour gas) is injected to the oil wells. Also, the gas condensate of the refinery (about 15,000 barrels/day) is directed to the Taheri harbor for exporting.

Since the Farashband refinery is close to Farashband city, finding a method to use flare gas of this refinery and prevent its emission to the atmosphere is very important. It is clear that this method should be not only clean for ecosystems near flare site but also economical and returns investment in proper time.

Therefore, in the present work, three practical options are devised with simulation and economic evaluation to reduce, recover and reuse flare gases for Farashband gas refinery.

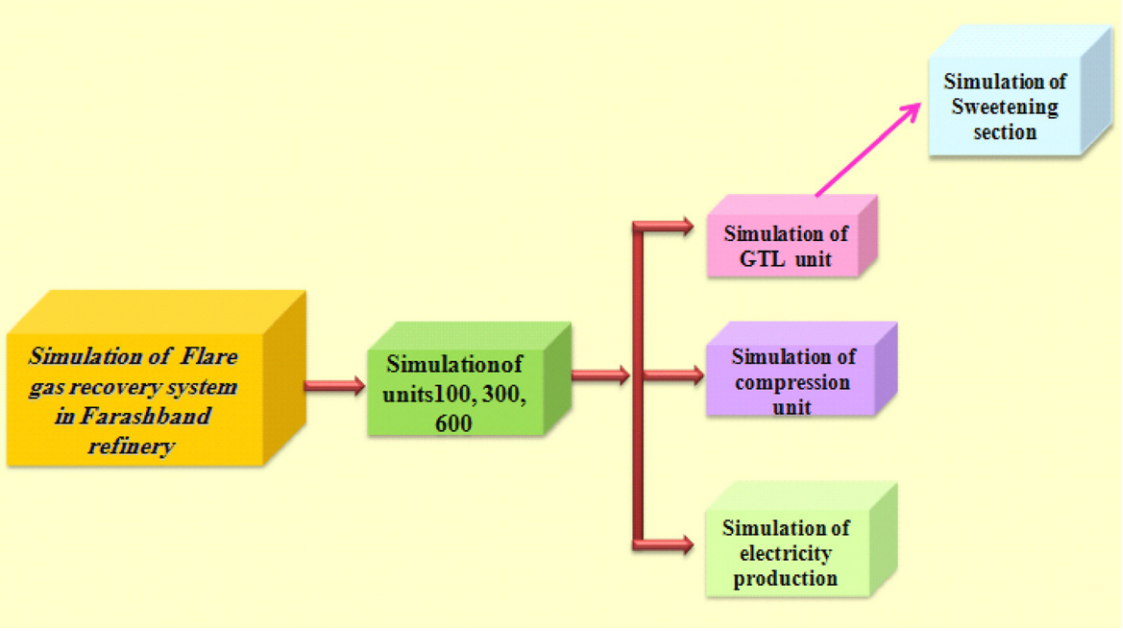

Fig. 1. The trend of simulations.

Table 1
Composition of streams in Fig. 2.

Component	Aghar	Dalan	V-105		V-101		V-100		T-101		
			Out 1	Out 2	Out 1	Out 2	Out 1	Out 2	TEG	Out 1	Out 2
Methane	0.897720	0.871123	0.902648	0.262678	0.880355	0.216265	0.903985	0.342821	0.000000	0.909714	0.038990
Ethane	0.014531	0.014046	0.014570	0.009552	0.014112	0.009364	0.014567	0.015559	0.000000	0.013490	0.001430
Propane	0.004301	0.003428	0.004295	0.005117	0.003410	0.004745	0.004282	0.009756	0.000000	0.003057	0.000495
Nitrogen	0.054538	0.077376	0.054890	0.009237	0.078324	0.010102	0.054997	0.010129	0.000000	0.059876	0.018978
CO_2	0.012976	0.016274	0.013021	0.007126	0.016384	0.008466	0.013029	0.009932	0.000000	0.008192	0.007161
H_2S	0.000070	0.000000	0.000070	0.000072	0.000000	0.000000	0.000070	0.000110	0.000000	0.000000	0.000000
i-Butane	0.001145	0.000967	0.001138	0.002086	0.000948	0.002272	0.001130	0.004418	0.000000	0.000957	0.000059
n-Butane	0.001722	0.001405	0.001707	0.003722	0.001368	0.004027	0.001691	0.008236	0.000000	0.001371	0.000091
C_5^+	0.008575	0.008271	0.006587	0.264509	0.003572	0.341567	0.005512	0.456707	0.000000	0.003335	0.923192
H_2O	0.004422	0.006781	0.001074	0.435901	0.001279	0.397129	0.000737	0.142332	0.009000	0.000008	0.009404
Benzene	0.000000	0.000120	0.000000	0.000000	0.000101	0.001448	0.000000	0.000000	0.000000	0.000000	0.000081
Toluene	0.000000	0.000209	0.000000	0.000000	0.000147	0.004615	0.000000	0.000000	0.000000	0.000000	0.000119
TEG	0.000000	0.000000	0.000000	0.000000	0.000000	0.000000	0.000000	0.000000	0.991000	0.000000	0.000000

2. Process description

The first step in this work is to calculate the amounts of flare gas and its composition. For this purpose, refinery units that send gas to the flare are simulated. These units are named units 100, 300 and 600 in Farashband refinery. The simulations are done by the steady state process simulation software (licensed by Oil Company with hardware lock of S/N 08225).

These data are used for simulation of GTL, compression and electricity generation options. The catalysts of GTL reactors are poisoned by hydrogen sulfide. Therefore, it is essential to remove it in sweetening unit before sending the flare gas to the GTL plant. The simulation of sweetening unit is carried out before GTL plant simulation. The simulation procedure is illustrated in Fig. 1.

2.1. Simulation of units 100, 600 and 300 of Farashband refinery

Figs. 2 and 3 show schematic diagram of simulation of units 100, 600 and 300. As it is shown in Fig. 2, gas stream from Aghar field with temperature 45 °C, pressure 181 bar and flow rate of 760.7 MMSCFD enters the sludge catcher of Aghar central facility (V-105). In unit 100 the gas phase of V-105 is directed to the Aghar sludge catcher (V-100). The pressure drop in the pipeline is simulated with a valve (VLV-102) in simulation software. The gas phase from V-100 is directed to unit 200 for dehydration and the liquid phase from V-105 is directed to three phase separator (V-108) to separate liquid, gas and water. The liquid phase enters the mixer (Mix-100). Also, gas stream from Dalan field with temperature 45 °C, pressure 129 bar and flow rate 707.6 MMSCFD enters the sludge catcher of Dalan (V-101) at the refinery entrance. Gas phase enters unit 600 (T-101) for dehydration with triethylene glycol (TEG) and the liquid phase is directed to the mixer (Mix-100). The output of Mix-100 is fed to unit 300. The dehydrated gas from dehydration column (T-101) enters the tube side of the gas/gas heat exchanger (E-101) to be pre-cooled by the cold gas coming out of the low temperature separator (V-107). The gas leaving E-101 is pre-cooled to approximately −2 °C. The cooled gas is then expanded across J–T valve (VLV-105) with a pressure reduction from 129 bar to 77.5 bar and the effect is cooling of the gas from −2 to −20 °C. Chilling the gas to this temperature at this pressure provides a H/C dewpoint of −15 °C at 71 bar. Output gases from V-100, V-101 and V-108 enter the gas mixer (Mix-101). The gas leaving Mix-101 with the gas leaving V-107 enters to a 3 phase separator (V-102) which is placed in unit 300. The gas phase from V-102 is directed to the flare. Outlet water of this three phase separator is discharged to a storage tank (V-104) and the liquid phase after pressure reduction with a valve (VLV-101) is directed to the next 3 phase separator (V-103) which is shown in Fig. 3. Also, the gas phase of this separator is directed to the flare and the liquid phase splits in two streams with the ratio of 0.25 and 0.75. The first stream is fed through the first tray of the stabilizer column (T-1000) and the second stream after heat exchanging with the output of column and rising its temperature is fed to the 6th tray of the column. The stabilizer has 15 trays and its heating system is a kettle type heat exchanger that its hot fluid is oil which is provided by a cylindrical burner. The gas from the column is directed to the burner and the liquid is directed to the Taheri harbor for exporting [52]. As Fig. 3 shows, gas is sent for flaring via three main streams; these streams are from V-102, V-103 and T-100. The operating conditions of these streams are illustrated in Figs. 2 and 3 where *T* is temperature (centigrade degrees), *P* is stream pressure (bar) and *F* is flow rate of stream (MMSCFD). The simulation shows 4.176 MMSCFD gas is gathered in flare. The composition and conditions of flare gas are reported in Tables 1 and 2.

Table 2
Composition of streams in Fig. 2 (continued).

Component	V-108			V-107		Mix- 100	V-102			V-106	
	Out 1	Out 2	Out 3	Out 1	Out 2	Out 2	Out 1	Out 2	Out 3	Out 1	Out 2
Methane	0.912376	0.253830	0.000001	0.910511	0.377890	0.238739	0.897754	0.151412	0.000000	0.897897	0.000000
Ethane	0.018030	0.016387	0.000000	0.013470	0.026736	0.011303	0.022857	0.015066	0.000000	0.022856	0.000000
Propane	0.004970	0.010993	0.000000	0.003033	0.018820	0.006406	0.006130	0.011352	0.000000	0.006129	0.000000
Nitrogen	0.040011	0.005150	0.000028	0.059953	0.008701	0.009304	0.041409	0.002934	0.000017	0.041419	0.000017
CO_2	0.016755	0.010343	0.000283	0.008189	0.010043	0.008960	0.022024	0.009107	0.000255	0.022025	0.000255
H_2S	0.000099	0.000134	0.000005	0.000000	0.000000	0.000036	0.000047	0.000046	0.000002	0.000047	0.000002
i-Butane	0.001148	0.004896	0.000000	0.000939	0.012984	0.002975	0.001558	0.006232	0.000000	0.001558	0.000000
n-Butane	0.001648	0.008925	0.000000	0.001335	0.025832	0.005365	0.002238	0.011728	0.000000	0.002238	0.000000
C_5^+	0.003128	0.688147	0.000000	0.002562	0.518984	0.412574	0.003624	0.783664	0.000001	0.003472	0.000001
H_2O	0.001835	0.001195	0.999683	0.000008	0.000010	0.300042	0.002260	0.000971	0.999725	0.002260	0.999725
Benzene	0.000000	0.000000	0.000000	0.000000	0.000000	0.001026	0.000046	0.001781	0.000000	0.000046	0.000000
Toluene	0.000000	0.000000	0.000000	0.000000	0.000000	0.003270	0.000053	0.005707	0.000000	0.000053	0.000000

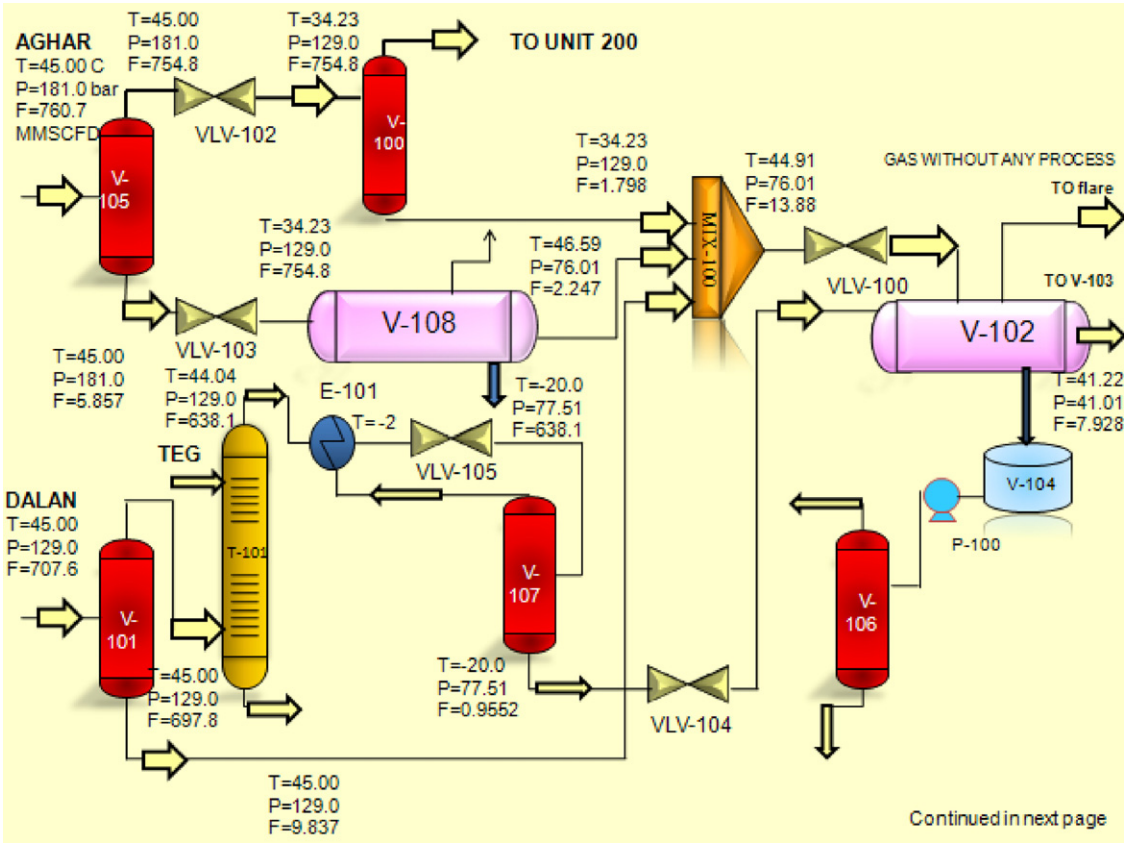

Fig. 2. Simulation of unit 100, 600 and 300 of Farashband refinery.

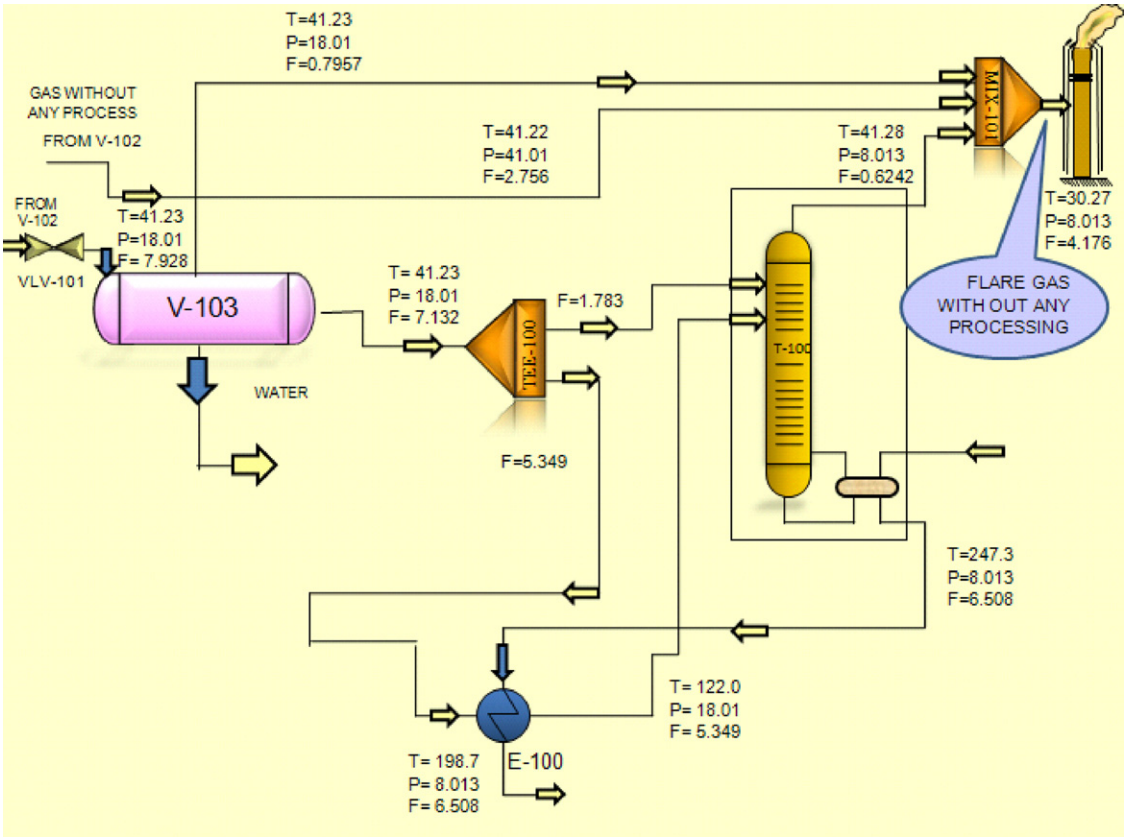

Fig. 3. Simulation of units 100, 600 and 300 of Farashband refinery (continued).

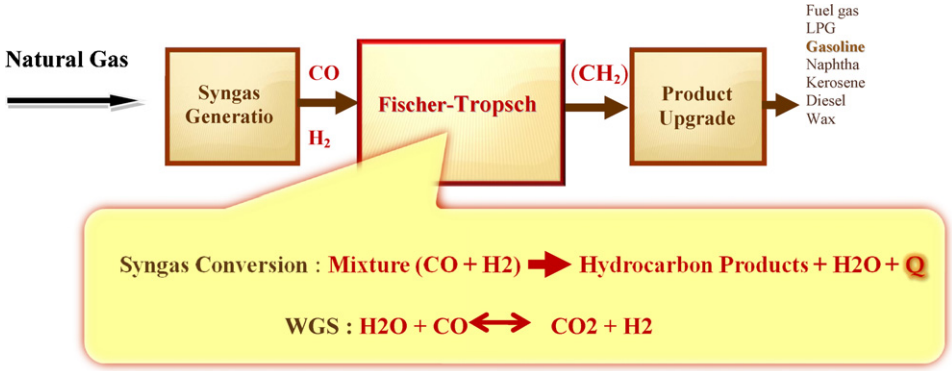

Fig. 4. Schematic diagram of main section of GTL technology.

2.2. Simulation of GTL option

Feed of GTL option is provided by different units which equals 4.176 MMCFD. The GTL technology consists of a chemical conversion of natural gas into a stable liquid by means of the Fischer–Tropsch (F–T) process. The commercial process consists of three main sections including synthesis gas (syngas) generation, Fischer–Tropsch synthesis and product upgrading. A schematic diagram of the main section of GTL technology, a process that initially converts natural gas to synthesis gas (a mixture of hydrogen and carbon monoxide) and then follows by a conversion process to liquid fuels, is illustrated in Fig. 4. The GTL process produces synthetic transportation fuels, zero-sulfur, fully fungible products and compatible with existing liquid fuels, which can be introduced into the current infrastructure and supply system. The syngas generation is a very important step in GTL production. In this stage, natural gas is converted into hydrogen and carbon monoxide by partial oxidation, steam reforming or a combination of these two processes (auto thermal reforming). In this study, the steam reforming is selected in the simulation process because the produced water as the by-product of GTL plant can be used for steam reforming. The GTL option is simulated in order to determine the number of produced GTL barrels from flare gas. Hydrogen sulfide content must be less than 4 ppm to prevent catalyst poisoning in steam reforming and the F–T reactors. Thus, hydrogen sulfide is removed from gas in sweetening unit before GTL plant. Fig. 5 shows the schematic diagram of simulation of sweetening unit. In this unit, Di Ethanol Amine (DEA) is used as an absorbent for gas sweetening. Flare gas, after compression and reaching to the appropriate pressure (68.94 bar), is fed to an absorber. The specifications of the absorber are determined to achieve the minimum content of hydrogen sulfide in sweetened gas. The scrubbed sweetened gas via DEA is transmitted by pipeline to GTL plant for further processing. The achieved rich DEA solution from the absorber is sent to a flash tank which operates at much lower pressures. In this step, any light-end hydrocarbons that are not captured in the absorber are removed. The light-end gases are sent for further processing. Subsequently, the hydrocarbon-free DEA is fed to a regeneration column. In this column, heat is applied to strip the acid gas components from DEA. Sour gas exits from the regeneration column and the regenerated DEA is recycled to the absorber. The characterization of each stream and the conditions of columns are shown in Fig. 5. The composition of gas after sweetening unit is reported in Table 3.

As shown in Fig. 6, the number of produced GTL barrels is determined by simulating the GTL option. The sweetened gas, after reaching to required temperature and pressure conditions, enters steam reforming reactor. The following equilibrium reactions take place in steam reforming reactor [53]:

$$CH_4 + H_2O \leftrightarrow CO + 3H_2 \quad \Delta H^\circ_{298K} = 205.92\,kJ/mol \tag{1}$$

$$CH_4 + CO_2 \leftrightarrow 2CO + 2H_2 \quad \Delta H^\circ_{298K} = 247.32\,kJ/mol \tag{2}$$

These equilibrium reactions take place in an equilibrium reactor (ERV-100) in the steady state process simulation software. The exited syngas from ERV-100 and the recycled gas from final unit are directed to the F–T reactor (PFR-100). It is worth mentioning that temperature is an important factor in FT reactor owing to the exothermic nature of these reactions. The Fischer–Tropsch components include H_2, CO, CO_2, H_2O, CH_4, C_2H_6, C_3H_8, n-C_4H_{10}, i-C_4H_{10} and C_5^+. The following reactions are considered as dominate FT reactions [54]:

$$CO + 3H_2 \xrightarrow{R1} CH_4 + H_2O \tag{3}$$

$$2CO + 4H_2 \xrightarrow{R2} C_2H_4 + 2H_2O \tag{4}$$

$$2CO + 5H_2 \xrightarrow{R3} C_2H_6 + 2H_2O \tag{5}$$

Table 3
Composition of streams in Fig. 3.

Component	V-103			TEE-100		T- 100		FLARE GAS
	Out 1	Out 2	Out 3	Out 1	Out 2	Out 1	Out 2	
Methane	0.882077	0.069895	0.000000	0.069895	0.017139	0.796697	0.000181	0.879662
Ethane	0.036853	0.012635	0.000000	0.012635	0.004888	0.083260	0.005861	0.034552
Propane	0.010885	0.011404	0.000000	0.011404	0.004542	0.022757	0.010315	0.009521
Nitrogen	0.022789	0.000718	0.000006	0.000718	0.000114	0.008206	0.000000	0.032899
CO_2	0.032131	0.006538	0.000253	0.006538	0.001595	0.060269	0.001385	0.029666
H_2S	0.000083	0.000042	0.000002	0.000042	0.000008	0.000203	0.000026	0.002357
i-Butane	0.002733	0.006622	0.000000	0.006622	0.003134	0.005407	0.006738	0.003377
n-Butane	0.003906	0.012600	0.000000	0.012600	0.005746	0.007730	0.013068	0.003200
C_5^+	0.005037	0.870535	0.000000	0.870535	0.958907	0.009010	0.953171	0.004608
H_2O	0.003351	0.000705	0.999739	0.000705	0.000058	0.006165	0.000181	0.000077
Benzene	0.000075	0.001971	0.000000	0.001971	0.000799	0.000146	0.002146	0.000067
Toluene	0.000080	0.006335	0.000000	0.006335	0.003070	0.000150	0.006928	0.000073

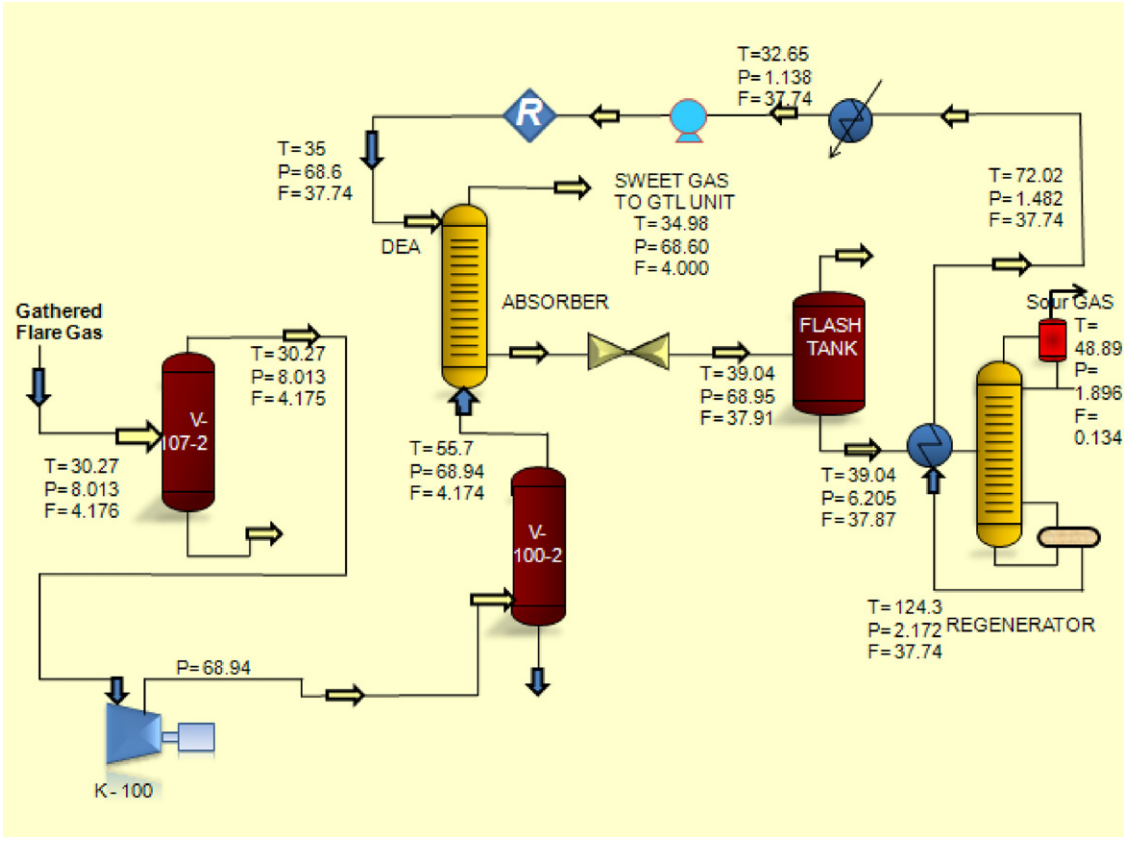

Fig. 5. Process flow diagram of sweetening unit simulation.

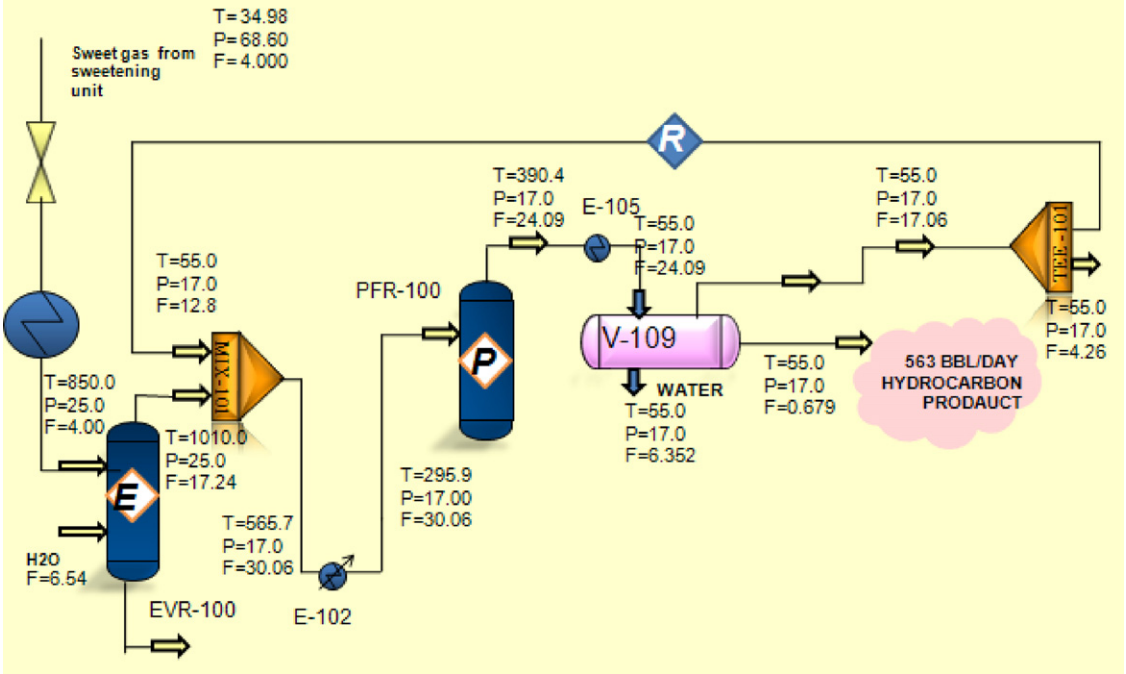

Fig. 6. Process flow diagram of GTL plant simulation.

Table 4
Comparison between industrial and simulation data of flare gas composition.

Component	Mole fraction (experimental) [52]	Mole fraction (simulation)	% Error
Methane	0.879662	0.884511	−0.55
Ethane	0.034552	0.036113	−4.51
Propane	0.009521	0.008912	6.39
Nitrogen	0.032899	0.029123	11.47
CO_2	0.029666	0.027512	7.26
i-Butane	0.002357	0.002898	−22.95
n-Butane	0.003377	0.003125	7.46
C_5^+	0.004608	0.004721	−2.45
H_2O	0.003052	0.002841	6.91
H_2S	0.000077	0.000080	−3.89
Benzene	0.000067	0.000072	−7.46
Toluene	0.000073	0.000078	−6.84

Table 5
Comparison between industrial and simulation data of flare gas conditions.

Conditions	Unit	Value (experimental) [52]	Value (simulation)	% Error
Temperature	C	30.27	27	−12.11
Pressure	kPa	801.3	750.0	−6.84
Molar flow	kg mol/h	208.0	200.0	−4.00
Mass flow	kg/h	3859	3710	−4.02

$$3CO + 7H_2 \xrightarrow{R4} C_3H_8 + 3H_2O \quad (6)$$

$$4CO + 9H_2 \xrightarrow{R5} n\text{-}C_4H_{10} + 4H_2O \quad (7)$$

$$4CO + 9H_2 \xrightarrow{R6} i\text{-}C_4H_{10} + 4H_2O \quad (8)$$

$$6.05CO + 12.23H_2 \xrightarrow{R7} C_{6.05}H_{12.36}(C_5^+) + 6.05H_2O \quad (9)$$

$$CO + H_2O \xrightarrow{R8} CO_2 + H_2 \quad \text{(WGS reaction)} \quad (10)$$

The reaction rate equation is as follows and the kinetic parameters are given in Table 4 [54].

$$R_i = 0.278 k_i \exp\left(\frac{-E_i}{RT}\right) P_{CO}^m \times P_{H_2}^n \quad (\text{mol/kg cat/s}) \quad (11)$$

The used kinetic model is valid for temperature range of 290–310 °C, pressure rang of 15–23 bars and H_2/CO ratio range of 0.76–1.82 [30]. The RIPI experimental data of GTL plant are used to simulate GTL option. The data of RIPI for steam reforming and F–T reactors are reported in Tables 5 and 6.

The outlet gas from F–T reactor is sent to the three phase separator after cooling. The gas phase is divided into two streams with the flow ratio of 0.75 and 0.25. The stream with higher flow rate is then recycled and the liquid phase is separated as GTL. According to the simulation results shown in Fig. 6, 563 barrels/day GTL is produced from GTL option. The obtained simulation results regarding syngas and GTL compositions are presented in Tables 7 and 8. It is noticeable that these products can be sent to petrochemical industry for hydro-cracking and product upgrading.

Table 6
Kinetic parameter data [54].

Reaction no.	*m*	*n*	*k*	*E*
(1)	−1.0889	1.5662	142583.8	83423.9
(2)	0.7622	0.0728	51.556	65018
(3)	−0.5645	1.3155	24.717	49782
(4)	0.4051	0.6635	0.4632	34885.5
(5)	0.4728	1.1389	0.00474	27728.9
(6)	0.8204	0.5026	0.00832	25730.1
(7)	0.5850	0.5982	0.02316	23564.3
(8)	0.5742	0.710	410.667	58826.3

Table 7
Pilot plant characteristics of steam reforming reactor.

System type	Pilot plant
Parameter	Value
Molar ratio of CH_4/H_2O in feed	0.55
Feed temperature [K]	850
Reactor pressure [bar]	25

2.3. Simulation of compression unit

Compression and gas injection to the refinery pipelines are proposed as the other alternative for reducing gas flaring. A compression unit is simulated in this regard. Some restrictions regarding materials limitation are considered during the simulation process. Considering proper materials for construction, sealing and lubrication, 150 °C is recommended as a "good average" for outlet temperatures [55]. The temperature range of 120–140 °C is recommended for operating under high pressures [55]. If the initial temperature is presumed close to the ambient temperature, pressure ratios of 3:1 to 5:1 are proposed by these maximum temperatures [55]. As shown in Figs. 7 and 8, three compressors are selected with considering the system design basis and flare gas recovery capacity. The inlet and outlet pressure are related, corresponding in the type of compressor and its configuration [51]. Fig. 9 shows different types of compressors. The most proper compressor for flare gas recovery depends on many factors such as process requirements, efficiency, dependability and maintenance requirements. In this simulation, the reciprocating compressor is selected [56]. A reciprocating compressor is a positive displacement machine in which the compressing and displacing element is a piston moving linearly within a cylinder [57]. As previously mentioned, gas is sent to flare by three lines therefore these streams are numbered as 1, 2 and 3 in Fig. 7. As shown in Fig. 7, the pressure of the streams 1 and 3 are increased via K-100 and K-101 compressors in order to reach the pressure of stream 2. Compressor K-100 is specified for the capacity of 0.7957 MMSCFD at the discharge pressure of 41 bar driven by a 33.20 kW, 35.28 rpm and compressor K-101 is specified for the capacity of 0.6242 MMSCFD at the discharge pressure of 41.01 bar driven by a 56.56 kW and 91.89 rpm. These streams are mixed together to form stream 4. As Fig. 8 shows, stream 4 passes through a cooler and enters the two phase separator. It is mentioned that this process is used to reduce the gas volume and materials limitation. The outlet gas pressure of separator is compressed to 129 bar by compressor K-102. Compressor K-102 is specified for the capacity of 4.176 MMSCFD at the discharge pressure of 129 bar driven by a 237.85 kW and 81.23 rpm. The characteristics of compressors K-100, K-101 and K-102 are presented in Table 9.

Table 8
FTS pilot plant characteristics.

System type	Pilot plant
Parameter	Value
Tube dimension [mm]	Ø 38.1 × 3 × 6000
Molar ratio of H_2/CO in feed	0.96
Feed temperature [K]	569
Reactor pressure [kPa]	1700
Cooling temperature [K]	566.2
Catalyst sizes [mm]	Ø 2.51 × 5.2
Catalyst density [kg/m^3]	1290
Bulk density [kg/m^3]	730
Number of tubes	1
GHSV [h^{-1}]	235
Bed voidage	0.488
Feed molar flow rate [g mol/s]	0.0335

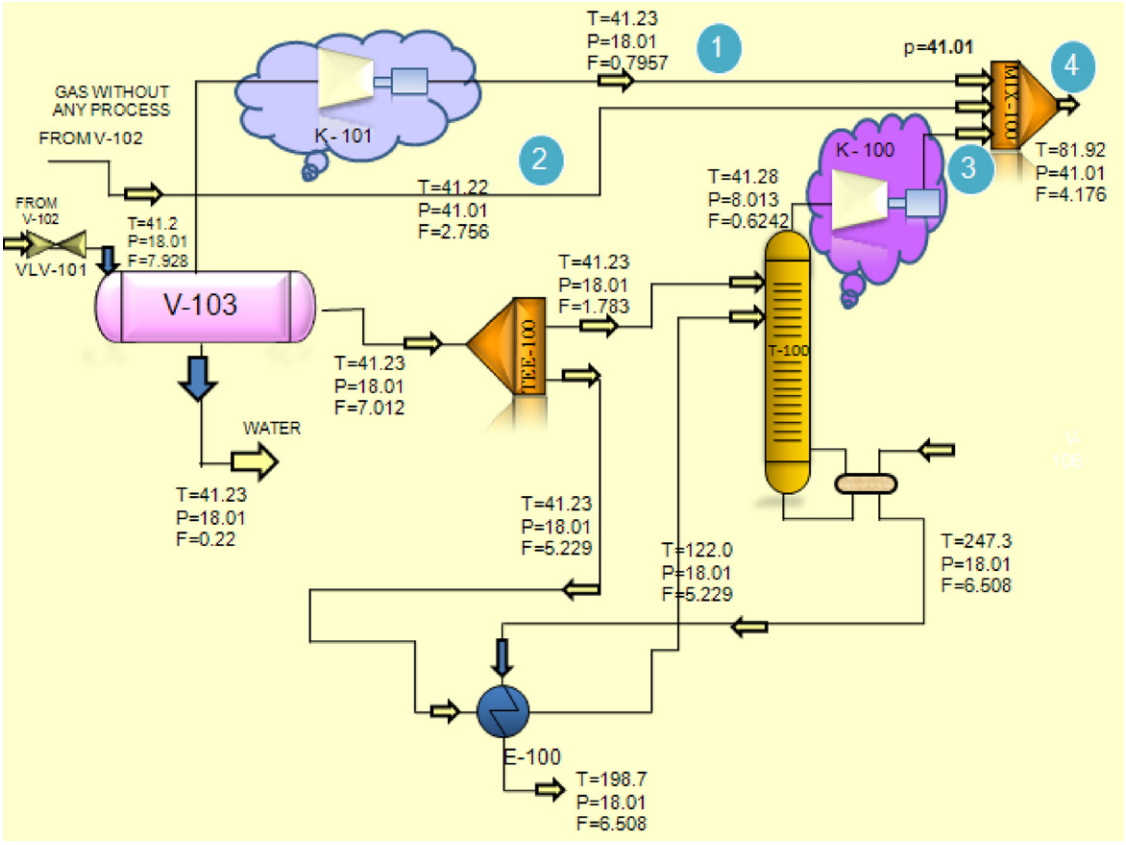

Fig. 7. Process flow diagram of compression unit simulation.

2.4. Simulation of electricity generation unit

The electricity generation with power cycle is the other way for eliminating gas flaring. The basic principle of the power cycle is simple: burning gas in a gas turbine (GT) produces power which can be converted to electric power by a coupled generator. This type of power plant is installed in increasing numbers around the world where substantial quantities of natural gas is abundant. This type of power plant produces high power outputs at high efficiencies and low emissions. Gas turbines have also been used in simple cycle mode for base load mechanical power and electricity generation in the oil and gas industries where natural gas and process gases have been used as fuel. The maintenance costs of gas fuels are lower than liquid fuels. The gas turbine cycle is best depicted by the

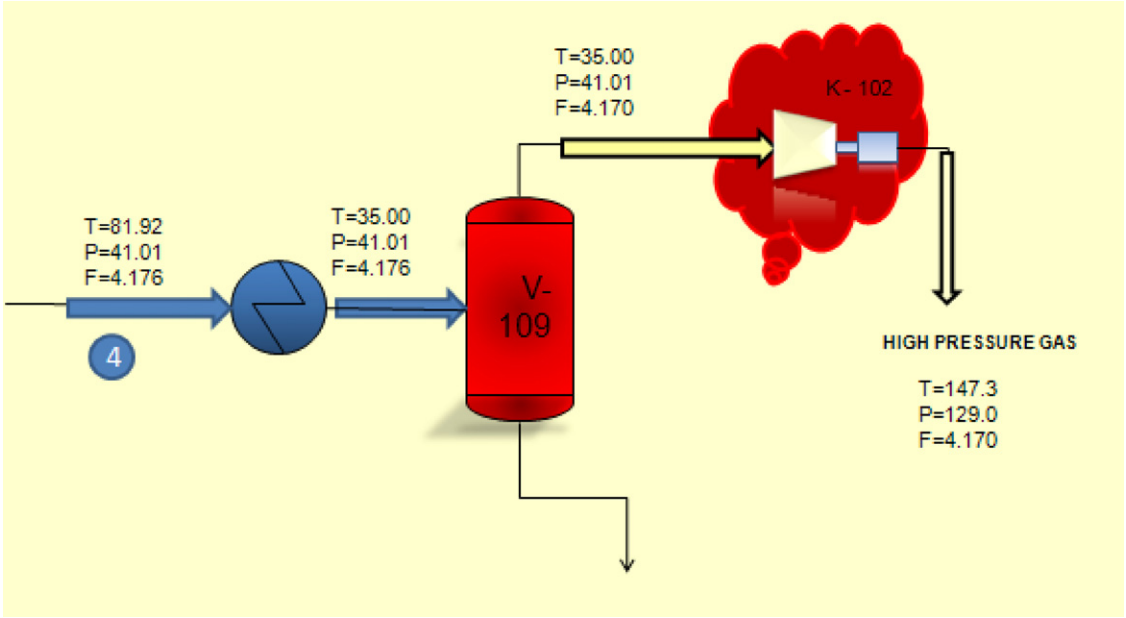

Fig. 8. Process flow diagram of compression unit simulation (continued).

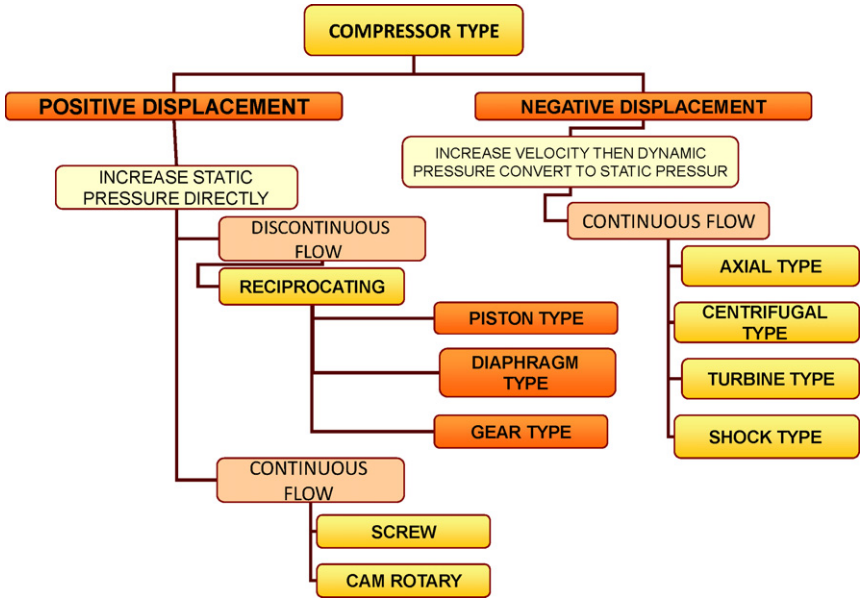

Fig. 9. The various types of compressors.

Brayton Cycle [58]. Fig. 10 shows Brayton cycle that is simulated in this study. The Brayton cycle is one of the most efficient cycles for the conversion of gas fuels to mechanical power or electricity. At point 1, the air which enters the plant comes from the atmosphere to the compressor where the pressure is increased from the atmospheric pressure to 23 bar. At point 2, the compressed air passes to a combustion chamber and it is blended with natural gas where combustion takes place. At point 3, the generated hot gases by combustion are directed to the gas turbine where they expand to the atmospheric pressure. The energy of gas is converted to mechanical energy and this energy converts into electricity in a generator. At point 4, the exhausted gases come out from the gas turbine. The obtained power by the electricity generation option is determined by the simulation. Fig. 11 shows the simulation of electricity generation option. The pressures of air and discharged flare gas from Farashband gas refinery are compressed to the pressure of combustion reaction by compressors K-100 and K-101. Afterward, the outlet gas enters the conversion reactor which is substituted by combustion chamber in the steady state process simulation software. The following reaction takes place in the reactor [59]:

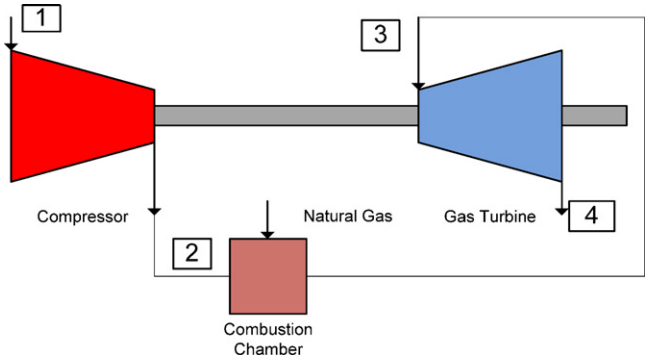

Fig. 10. The Brayton cycle.

$$CH_4 + 2O_2 \leftrightarrow CO_2 + 2H_2O \quad \Delta H^{\circ}_{298K} = 800\,kJ/mol \tag{12}$$

The outlet gas stream from the reactor is directed to the gas turbine (T-100). As Fig. 11 shows, 25 MW power is obtained by electricity generation option. The characteristics of gas turbine (T-100) are identified in Table 10.

3. Economic evaluation

In this case, the investment decision is based on a comparison between three alternatives such as GTL technology, gas compression and electricity generation. After simulating three aforementioned processes via the steady state process simulation software, an economic assessment of each process is evaluated.

Table 9
Composition of streams in sweetening unit.

Component	V-107-2		V-100-2		Absorber		Flash tank			Sour gas
	Out 1	Out 2	Out 1	Out 2	DEA	Sweet gas	in	Out 1	Out 2	
Methane	0.879665	0.033298	0.880110	0.000001	0.000000	0.907894	0.001108	0.931430	0.000117	0.032852
Ethane	0.034552	0.006633	0.034569	0.000000	0.000000	0.035719	0.000037	0.031051	0.000004	0.001217
Propane	0.009521	0.006274	0.009526	0.000000	0.000000	0.009877	0.000007	0.005747	0.000001	0.000182
Nitrogen	0.032899	0.000445	0.032915	0.000020	0.000000	0.034131	0.000023	0.020310	0.000001	0.000345
CO_2	0.029666	0.003155	0.029681	0.000414	0.001491	0.000681	0.003988	0.000036	0.003992	0.900150
H_2S	0.000077	0.000022	0.000077	0.000003	0.000006	0.002460	0.000013	0.000001	0.000013	0.002338
i-Butane	0.002357	0.003896	0.002358	0.000000	0.000000	0.003525	0.000000	0.000056	0.000000	0.000000
n-Butane	0.003377	0.007680	0.003379	0.000000	0.000000	0.001469	0.000000	0.000076	0.000000	0.000000
C_5^+	0.004694	0.931191	0.004192	0.000000	0.280083	0.003210	0.062280	0.000220	0.062348	0.000001
H_2O	0.003052	0.000332	0.003053	0.999562	0.718420	0.001215	0.932542	0.010742	0.933523	0.062478
Benzene	0.000067	0.001521	0.000067	0.000000	0.000000	0.000054	0.000002	0.000218	0.000001	0.000401
Toluene	0.000073	0.005553	0.000073	0.000000	0.000000	0.000073	0.000000	0.000113	0.000000	0.000036

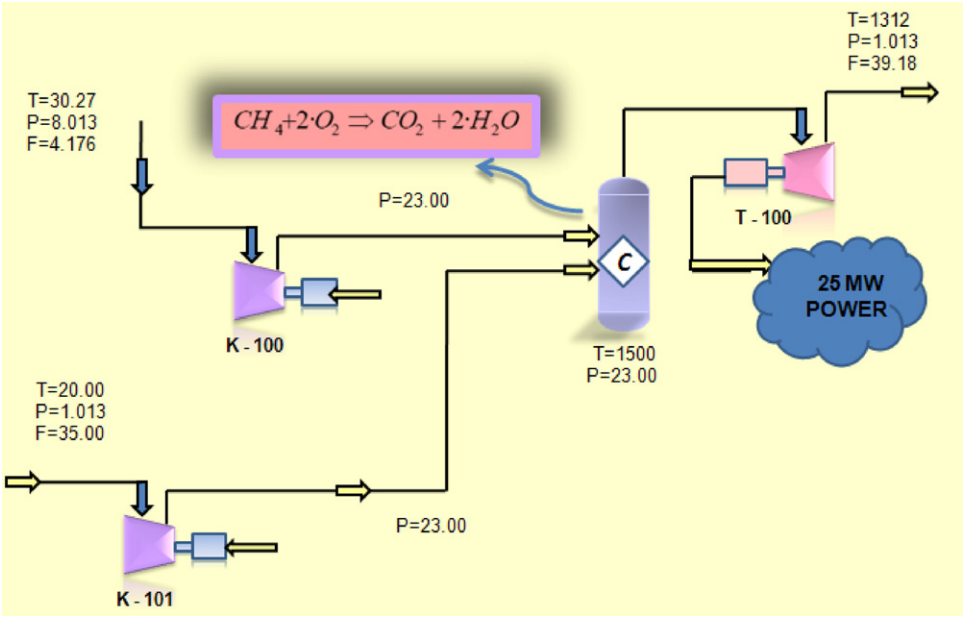

Fig. 11. Process flow diagram of power plant simulation.

Table 10
Composition of streams in GTL plant.

Component	EVR-100			PFR-101		V-109			TEE-101	
	H_2O	Out 1	Out 2	in	Out	Out 1	Out 2 (GTL)	Out 3	Out 1	Out 2
Methane	0.000000	0.016566	0.016566	0.037230	0.046428	0.065081	0.010735	0.000000	0.065081	0.065081
Ethane	0.000000	0.008288	0.008288	0.014420	0.018041	0.022678	0.058860	0.000000	0.022678	0.022678
Propane	0.000000	0.002292	0.002292	0.002198	0.002880	0.002073	0.046706	0.000000	0.002073	0.002073
Nitrogen	0.000000	0.007920	0.007920	0.018028	0.022477	0.031652	0.000899	0.000134	0.031652	0.031652
CO_2	0.000000	0.025754	0.025754	0.018860	0.007662	0.009573	0.009399	0.002156	0.009573	0.009573
CO	0.000000	0.168505	0.168505	0.106235	0.015857	0.022350	0.000965	0.000000	0.022350	0.022350
H_2	0.000000	0.607900	0.607900	0.709234	0.599082	0.845726	0.006226	0.000001	0.845726	0.845726
i-Butane	0.000000	0.000571	0.000571	0.000547	0.001841	0.000515	0.051886	0.000000	0.000515	0.000515
n-Butane	0.000000	0.000818	0.000818	0.000543	0.001025	0.000174	0.032094	0.000000	0.000174	0.000174
C_5^+	0.000000	0.001013	0.001013	0.000657	0.021648	0.000176	0.755199	0.000000	0.000176	0.000176
Ethylene	0.000000	0.000000	0.000000	0.000000	0.000000	0.000000	0.000111	0.000000	0.000000	0.000000
H_2O	1.000000	0.160343	0.160343	0.092031	0.263038	0.000002	0.000005	0.997710	0.000002	0.000002
Benzene	0.000000	0.000013	0.000013	0.000007	0.000009	0.000000	0.000325	0.000000	0.000000	0.000000
Toluene	0.000000	0.000017	0.000017	0.000010	0.000012	0.000000	0.000443	0.000000	0.000000	0.000000

The profitability of each process is analyzed using rate of return for capacity increment (ROR). It is observed that the feedstock gas cost of GTL technology has an impact on GTL plant cost because it depends widely on alternative applications. The cost of natural gas used as an inlet feed of the GTL plant leads to an increase in GTL option costs; however, the flare gas is used as an inlet feed in this study and consequently costs regarding natural gas feed are eliminated. In other words, the cost of GTL plant with flare gas is less than the same plant with natural gas. The cost of each process is reported in the following tables. The equipment cost is shown in Table 11.

Estimated capital investment for producing 563 barrels/day liquid fuel with GTL technology, income and return statement are reported in Table 12.

These calculations imply that the period of return on investment for GTL option is about 3 years and 9 months (100/27 = 3.7 years) and total net profit is $9,054,864/year. Estimated capital

Table 11
The characteristics of compressors K-100, K-101 and K-102.

Compressors name	K-100	K-101	K-102
Adiabatic head (m)	12375.19	24077.57	16995.36
Polytropic head (m)	12702.99	25057.57	17609.47
Adiabatic efficiency	75.00	75.00	75.00
Polytropic efficiency	77.01	78.25	77.71
Power consumed (kW)	33.20	56.56	237.85
Friction loss (kW)	0.00	0.00	0.00
Fluid power (kW)	33.20	56.56	237.85
Polytropic head factor	1.00	1.00	0.99
Polytropic exponent	1.38	1.31	51.4
Isentropic exponent	1.27	1.23	1.33
Speed (rpm)	35.28	91.89	81.23

Table 12
The characteristics of gas turbine (T-100).

Gas turbine name	T-100
Adiabatic head (m)	182723.06
Polytropic head (m)	184919.83
Adiabatic efficiency	93.00
Polytropic efficiency	90.44
Power consumed (kW)	25067.11
Friction loss (kW)	0.00
Fluid power (kW)	25067.11
Polytropic head factor	1.00
Polytropic exponent	1.20
Isentropic exponent	1.23

Table 13
The main equipment approximate cost.

Items	Equipment	Cost
1.	Reciprocating compressor	$301,000
2.	Reactor	$3,864,300
3.	DEG contactor	$956,200
4.	Two phase separator	$115,300
5.	Three phase separator	$256,000
6.	Heat exchanger	$60,100

Table 14
Estimated capital investment, income and return cost statement for GTL plant.

Items	Caption	Value
1.	Purchased equipment cost	$11,345,267
2.	Total direct cost	$20,421,480
3.	Total indirect cost	$6,126,444
4.	Total fixed cost	$26,547,924
5.	Working cost	$6,807,160
6.	Total capital investment	$33,355,084
7.	Product cost for sale 500 bbl/day	$90/bbl
8.	Gross profit	$1,138,580/year
9.	Net profit	$9,054,864/year
10.	ROR	27%

investment, income and return statement for compression of 4.176 MMSCFD flare gas are presented in Table 13.

These calculations show that the period of return on investment for compression unit is about 2 years and 10 months (100/36 = 2.8 years) and net profit is $1,225,510/year. Table 14 presents estimated capital investment, income and return statement for 25 MW electricity generation (Table 15).

These calculations show that the period of return on investment for electricity generation option is 2 years and 4 months (100/44 = 2.3 years) and net profit is $14,053,600/year (Table 16).

Table 15
Estimated capital investment, income and return cost statement for compression unit.

Items	Caption	Cost
1.	Purchased equipment cost	$800,000
2.	Total direct cost	$2,160,000
3.	Total indirect cost	$560,000
4.	Total fixed cost	$2,720,000
5.	Working cost	$640,000
6.	Total capital investment	$3,360,000
7.	Product cost for sale 500 bbl/day	$0.06/m^3
8.	Gross profit	$1,531,888/year
9.	Net profit	$1,225,510/year
10.	ROR	36%

Table 16
Estimated capital investment, income and return cost statement for electricity generation.

Items	Caption	Cost
1.	Purchased equipment cost	$17,800,000
2.	Total direct cost	$24,860,000
3.	Total indirect cost	$3,520,000
4.	Total fixed cost	$28,380,000
5.	Working cost	$3,560,000/year
6.	Total capital investment	$31,940,000
7.	Product cost for sale 500 bbl/day	$0.12/kWh
8.	Gross profit	$21,958,750/year
9.	Net profit	$14,053,600/year
10.	ROR	44%

The break – even point capacity (B.E.P.), product cost for plant, yearly income in B.E.P. capacity, total yearly income, gross profit, net profit and ROR are calculated by using Eqs. (13)–(19) [60].

$$\text{product cost for sale} \times \text{B.E.P. capacity} = [\text{product cost for plant} \times \text{B.E.P. capacity} + \text{fixed charge} \quad (13)$$

$$\text{product cost for plant} = \frac{\text{direct production cost}}{\text{plant capacity}} \quad (14)$$

$$\text{yearly income in B.E.P. capacity} = \text{break} - \text{even point capacity} \times \text{product cost for sale} \quad (15)$$

$$\text{total yearly income} = \text{capacity of unit per year} \times \text{product cost for sale} \quad (16)$$

$$\text{gross profit} = \text{total yearly income} - \text{yearly income in B.E.P. capacity} \quad (17)$$

$$\text{net profit} = 0.8 \times \text{gross profit} \quad (18)$$

$$\text{ROR} = \frac{\text{annual profit}}{\text{capital investment}} \times 100 \quad (19)$$

According to the above mentioned calculations, a comparison between capital investments, annual profits, ROR and payback period of three methods are shown in Figs. 12, 13, 14 and 15, respectively.

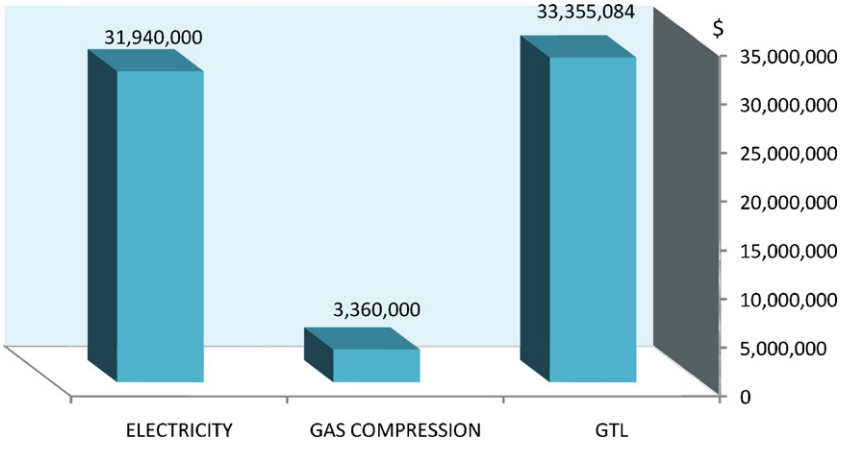

Fig. 12. A comparison between total capital investments.

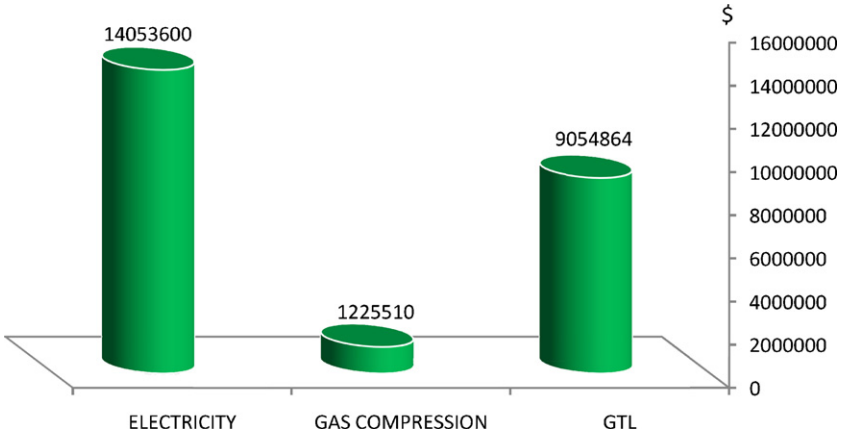

Fig. 13. A comparison between annual profits.

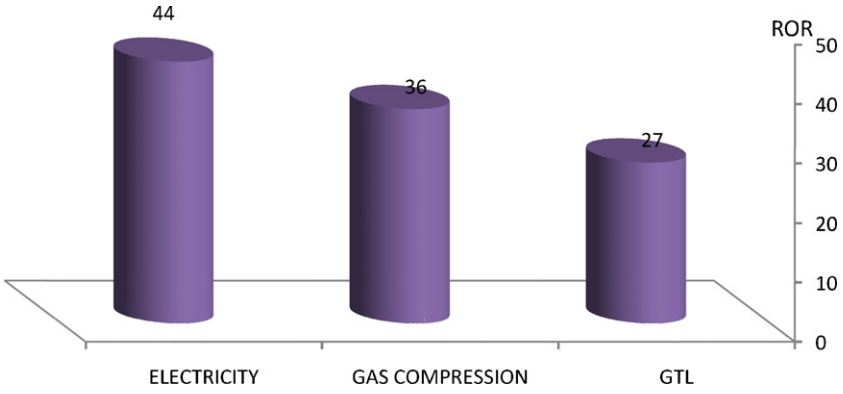

Fig. 14. A comparison between rates of return for capacity increment.

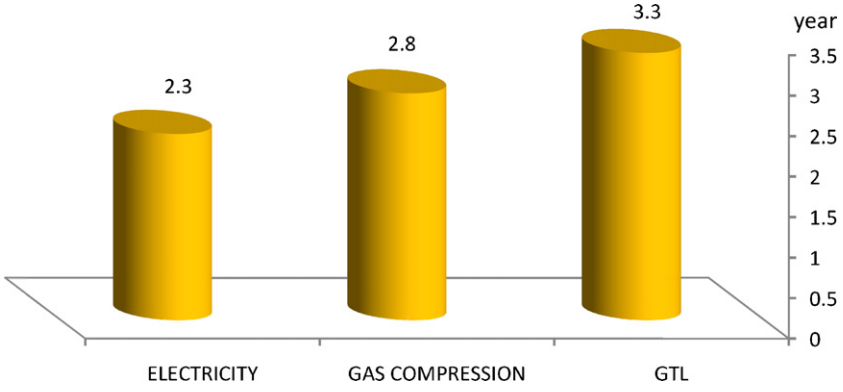

Fig. 15. A comparison between payback period.

The economic evaluation of three methods is compared in the following figures. Although each method has its own advantage owing to preventing gas flaring and consequent problems, a comparison is made to recognize the superior method economically.

A comparison of total capital investments for the three methods is shown in Fig. 12. It can be seen that the gas compression has the lowest capital investment. Fig. 13 shows that the annual profit for electricity is higher than that of GTL and the annual profit for GTL is higher than that of gas compression. However, electricity generation corresponds to the lowest payback period due to higher ROR compared to GTL plant and gas compression options (see Fig. 14). A comparison between Figs. 14 and 15 shows that the highest return for capacity increment and the lowest payback period correspond to the electricity generation method (see Figs. 14 and 15).

4. Conclusions

Gas flaring in gas refineries produces a great amount of hazardous materials in the atmosphere. There are many methods for minimizing purge gas flaring in oil and gas refineries. In order to determine a suitable method for minimizing gas flaring in Farashband gas refinery, a comprehensive monitoring of flow and composition of flare gases and alternative choices for recovery of flare gases were investigated in this study. To this end, process simulations, process evaluations and economical evaluations were carried out for three alternatives such as electricity generation, GTL and reinjection of compressed gas into the refinery. The simulation results demonstrated that that the gas to electricity generation option (with 4.176 MMSCFD of flare gas) required mild capital

investment and resulted in the highest annual profit. The gas to electricity option also gave the highest rate of return on investment (44%) as well as the lowest payback period among the three alternatives (2.3 years) so that it is the most appropriate method economically. The Gas to Liquid option corresponded to lower ROR (27%) and higher capital investment than the other methods, a fact that shows it is the least attractive method. Although capital investment for the compression unit was low, the rate of return on investment was in second place (36%) and it renders the lowest annual profit. The comparisons show that electricity generation is the superior method economically.

Acknowledgements

The authors thank Research Institute of Petroleum Industry of Iran (RIPI) for providing the valuable pilot plant data. Also, the authors would like to appreciate South Zagros Oil and Gas Production Company for providing the data of Farashband gas refinery.

References

[1] M.R. Rahimpour, K. Alizadehhesari, Enhancement of carbon dioxide removal in a hydrogen perm-selective methanol synthesis reactor, Int. J. Hydrogen Energy 34 (2009) 1349–1362.
[2] A.O. Tolulope, Oil exploration and environmental degradation: the Nigerian experience, Environ. Inform. Arch. 2 (2004) 387–393.
[3] C. Tanna, Worldwide gas flaring, in: Présentation pour la 2eme Conference du GGFR, Banque Mondiale, 2004.
[4] C.I. Soeze, News and trends, Africa 8 (2003) 21.
[5] K. Chakib, New Projects 2002–2006, in: Présentation pour la 2eme Conférence du GGFR, Banque Mondiale, 2004.
[6] N. Bjorndalen, S. Mustafiz, M.H. Rahman, M.R. Islam, No-flare design: converting waste to value addition, Energy Sources 27 (2005) 371–380.
[7] D. Mourad, O. Ghazi, B. Noureddine, Recovery of flare gas through crude oil stabilization by a multi-staged separation with intermediate feeds: a case study, Korean J. Chem. Eng. 26 (6) (2009) 1706–1716.
[8] Q. Xu, X. Yang, C. Liu, K. Li, H.H. Lou, J.L. Gossage, Chemical plant flare minimization via plantwide dynamic simulation, Ind. Eng. Chem. Res. 48 (2009) 3505–3512.
[9] G.C. Oguejiofor, Gas flaring in Nigeria: some aspects for accelerated development of SasolChevron GTL plant at Escravos, Energy Sources, Part A 28 (2006) 1365–1376.
[10] O. Zadakbar, A. Vatani, K. Karimpour, Flare gas recovery in oil and gas refineries, Oil Gas Sci. Technol. – Rev. IFP 63 (2008) 705–711.
[11] E. Cairncross, Report and technical protocol for the monitoring and regulation of flaring from oil refineries in South Africa, UEM flaring project final report, 2007.
[12] A. Ezersky, H. Lips, Characterisation of Refinery Flare Emissions: Assumptions, Assertions and AP-42, Bay Area Air Quality Management District (BAAQMD), 2003.
[13] US EPA Enforcement Alert, vol. 3, No. 9, 2000.
[14] A. Ezersky, B. Guy, Proposed regulation 12, Rule 11: Flare Monitoring at Petroleum Refineries, 2003.
[15] C.R. Mohantyb, Sivaji Adapalaa, B.C. Meikapa, Removal of hazardous gaseous pollutants from industrial flue gases bya novel multi-stage fluidized bed desulfurizer, J. Hazard. Mater. 165 (2009) 427–434.
[16] I. Mochida, Y. Koraia, M. Shirahama, S. Kawano, T. Hada, Y. Seo, M. Yoshikawa, A. Yasutake, Removal of SO and NO over activated carbon fibers, Carbon 38 (2000) 227–239.
[17] J. Miles, Zero flaring can achieve operational environmental benefits, Oil Gas J. 30 (2001) 72–75.
[18] IPCC Climate Change – The Scientific Basis, Cambridge University Press, Cambridge 2001.
[19] M. Rydén, A. Lyngfelt, T. Mattisson, $CaMn_{0.875}Ti_{0.125}O_3$ as oxygen carrier for chemical-looping combustion with oxygen uncoupling (CLOU) Experiments in a continuously operating fluidized-bed reactor system, Int. J. Greenhouse Gas Control 5 (2011) 356–366.
[20] B. Hileman, An urgent plea on global warming, Chem. Eng. News 82 (26) (2004) 44.
[21] Methanex, 2004 (http://www.methanex.com).
[22] M.R. Rahimpour, A two-stage catalyst bed concept for conversion of carbon dioxide into methanol, Fuel Process. Technol. 89 (2008) 556–566.
[23] G. Zahedi, A. Elkamel, A. Lohi, A. Jahanmiri, M.R. Rahimpor, Hybrid artificial neural network—first principle model formulation for the unsteady state simulation and analysis of a packed bed reactor for CO_2 hydrogenation to methanol, Chem. Eng. J. 115 (2005) 113–120.
[24] M.R. Rahimpour, H.R. Mottaghi, Simultaneous removal of urea, ammonia, and carbon dioxide from industrial wastewater using a thermal hydrolyzer-separator Loop, Ind. Eng. Chem. Res. 48 (22) (2009) 10037–10046.
[25] M.R. Rahimpour, A.Z. Kashkooli, Enhanced carbon dioxide removal by promoted hot potassium carbonate in a split-flow absorber, Chem. Eng. Process. 43 (2004) 857–865.
[26] W. Broere, The elusive goal to stop flares, Shell World, 2008, http://www.shell.com.
[27] M.R. Rahimpour, A. Asgari, Production of hydrogen from purge gases of ammonia plants in a catalytic hydrogen-permselective membrane reactor, Int. J. Hydrogen Energy 34 (2009) 5795–5802.
[28] H. Schulz, Short history and present trends of Fischer–Tropsch synthesis, Appl. Catal. A: Gen. 186 (1999) 3–12.
[29] L. Iandoli, S. Kjelstrup, Energy analysis of a GTL process based on low-temperature slurry FT reactor technology with a cobalt catalyst, Energy Fuels 21 (2007) 2317–2324.
[30] Fischer–Tropsch Pilot Plant of Research Institute of Petroleum Industry and National Iranian Oil Company (RIPINIOC), Tehran 18745-4163, Iran, 2004.
[31] M.A. Marvast, M. Sohrabi, S. Zarrinpashneh, Gh. Baghmisheh, Fischer–Tropsch synthesis: modeling and performance study for Fe-HZSM5 bifunctional catalyst, Chem. Eng. Technol. 28 (1) (2005) 78–86.
[32] M.R. Rahimpour, H. Elekaei, Optimization of a novel combination of fixed and fluidized bed hydrogen permselective membrane reactors for Fischer–Tropsch synthesis in GTL technology, Chem. Eng. J. 152 (2009) 543–555.
[33] M.R. Rahimpour, H. Elekaei, A comparative study of combination of Fischer–Tropsch synthesis reactors with hydrogen-permselective membrane in GTL technology, Fuel Process. Technol. 90 (2009) 747–761.
[34] A.A. Forghani, H. Elekaei, M.R. Rahimpour, Enhancement of gasoline production in a novel hydrogen permselective membrane reactor in Fischer–Tropsch synthesis of GTL technology, Int. J. Hydrogen Energy 34 (2009) 3965–3976.
[35] M.R. Rahimpour, K. Alizadehhesari, A novel fluidized-bed membrane dual-type reactor concept for methanol synthesis, Chem. Eng. Technol. 31 (2008) 1775–1789.
[36] M.R. Rahimpour, A. Mirvakili, K. Paymooni, A novel water perm-selective membrane dual-type reactor concept for Fischer–Tropsch synthesis of GTL (gas to liquid) technology, Energy 36 (2011) 1223–1235.
[37] M.R. Rahimpour, A. Mirvakili, K. Paymooni, Simultaneous hydrogen production and utilization via coupling of Fischere–Tropsch synthesis and decalin dehydrogenation reactions in GTL technology, Int. J. Hydrogen Energy 36 (4) (2011) 2992–3006.
[38] M.R. Rahimpour, A. Mirvakili, K. Paymooni, Differential evolution (DE) strategy for optimization of hydrogen production and utilization in a thermally coupled membrane reactor for decalin dehydrogenation and Fischer–Tropsch synthesis in GTL technology, J. Hydrogen Energy 36 (8) (2011) 4917–4933.
[39] L. Bregnbæk, C. Schaumburg-Müller, Local CHP plants between the natural gas and electricity systems, in: RISØ International Energy Conference, Denmark, 2005.
[40] Technical Manual TM 5-811-6, Electric Power Plant Design, Department of the Army, Washington, DC, USA, 1984.
[41] J. Požívil, Use of expansion turbines in natural gas pressure reduction stations, Acta Montan. Slov. 9 (3) (2004) 258.
[42] P.P. Walsh, P. Fletcher, Gas Turbine Performance, Royal Society/Blackwell Science, Oxford, 1998.
[43] J.H. Horlock, Cogeneration – Combined Heat and Power Plants, 2nd ed., Pergamon, Krieger, 1987.
[44] J.H. Horlock, Combined Power Plants, 2nd ed., Krieger, Pergamon, Melbourne, USA, 2002.
[45] J. Hodge, Cycles and Performance Estimation, Buttenvaths, London, 1955.
[46] H. Cohen, G.F.C. Rogers, H.I.H. Saravanamuttoo, Gas Turbine Theory, 4th ed., Longman, London, 1996.
[47] J. Kerrebrock, Aircraft Engines and Gas Turbines, MIT Press, 1992.
[48] J.H. Horlock, Advanced Gas Turbine Cycles, 1st ed., Elsevier Science Ltd., Cambridge, U.K, 2003.
[49] H. Dale Beggs, Gas Production Operations, Oil & Gas Consultants International Inc., 1984.
[50] P.W. Fisher, D. Brennan, Minimize flaring with flare gas recovery, 2002 (http://www.johnzink.com).
[51] R.N. Brown, Compressors: Selection and Sizing, 3rd ed., Elsevier Science & Technology Books, 2005.
[52] Farashband Gas Refinery data from Zagros Oil and Gas Company, Shiraz, Iran, 2010.
[53] P. Kiameh, Power Generation Handbook, 1st ed., McGraw-Hill, New York, NY, 2002.
[54] M.M. Montazer Rahmati, M. Bargah-Soleimani, Rate equations for the Fischer–Tropsch reaction on a promoted iron catalyst, Can. J. Chem. Eng. 79 (5) (2001) 800–804.
[55] A.J. Kidnay, W.R. Parrish, Fundamentals of Natural Gas Processing, Taylor and Francis, Ohio, 2006.
[56] http://www.atlascopco.com.
[57] S. Mokhatab, W.A. Poe, J.G. Speight, Handbook of Natural Gas Transmission and Processing, Elsevier, USA, 2006.
[58] T. Giampaolo, Gas Turbine Handbook: Principles and Practices, 3rd ed., The Fairmont Press, 2006.
[59] A.P. Steynberg, M.E. Dry, Fischer–Tropsch technology Studies in Surface Science and Catalysis, vol. 152, 1st ed., Elsevier, Amsterdam, The Netherlands, 2004.
[60] M.S. Peters, D. Timmerhaus, Plant Design and Economics for Chemical Engineering, 3rd ed., McGraw-Hill, New York, NY, 1981.